

An unbiased Monte Carlo estimator for derivatives. Application to CIR.

Victor Reutenauer¹ and Etienne Tanré²

¹Fotonower, France.

²Université Côte d’Azur, Inria, France.

January 27, 2023

Abstract

In this paper, we present extensions of the exact simulation algorithm introduced by Beskos et al. [2]. First, a modification in the order in which the simulation is done accelerates the algorithm. In addition, we propose a truncated version of the modified algorithm. We obtain a control of the bias of this last version, exponentially small in function of the truncation parameter. Then, we extend it to more general drift functions. Our main result is an unbiased algorithm to approximate the two first derivatives with respect to the initial condition x of quantities with the form $\mathbb{E}\Psi(X_T^x)$. Finally, we apply the algorithm to the CIR process and perform numerical tests to compare it with classical approximation procedures.

Keywords: Unbiased Monte Carlo methods; Monte Carlo Approximation of Derivatives; Exact Simulation of SDE.

AMS2010 class: 65C05, 60J60.

1 Introduction

In this paper, we are interested in the approximation of the law of a one dimensional stochastic process $(X_t^x, t \geq 0)$, defined as the unique solution of a Stochastic Differential Equation (SDE)

$$X_T^x = x + \int_0^T \alpha(X_t^x)dt + \int_0^T \sigma(X_t^x)dW_t, \quad (1)$$

with smooth coefficients α and σ . Let Ψ be a measurable function. The quantities we aim to evaluate take form

$$P_\Psi(x) := \mathbb{E}\Psi(X_T^x). \quad (2)$$

We also evaluate their sensitivities to the parameters of the model. We are especially interested in the dependance on the initial condition x ,

$$\Delta_\Psi(x) := \frac{d}{dx} \mathbb{E}\Psi(X_T^x) \quad (3)$$

$$\Gamma_\Psi(x) := \frac{d^2}{dx^2} \mathbb{E}\Psi(X_T^x). \quad (4)$$

These two derivatives are known as Delta and Gamma in the context of financial mathematics.

The most simple method to approximate (2) consists in a time discretization (say with step δ) of (1) with an Euler scheme. For an approximation of (3) or (4), one should evaluate (2) with two or three values, say for $x - dx$, x and $x + dx$. Then, we use a finite difference approximation of the derivatives. This method is very simple to implement, but we have three sources of error:

- 1) two biases due to
 - a - the time discretization;
 - b - the finite difference approximation;
- 2) the statistical error.

In [3] and [2], the authors proposed an exact simulation algorithm for one dimensional SDE with constant diffusion coefficient (see Section 2.1). This method removes the bias of type a- in the approximation of $P_\Psi(x)$.

Otherwise, in [5] the Malliavin calculus theory is developed to obtain expression of the derivatives $\Delta_\Psi(x)$ and $\Gamma_\Psi(x)$ without bias of type b-

$$\frac{d}{dx} \mathbb{E}[\Psi(X_T^x)] = \mathbb{E}[\Psi(X_T^x)H_T],$$

where H_T is an explicit random weight.

In this paper, we extend Beskos et al method of simulation: we simulate the Poisson process by ordering the points in increasing ordinate (see Sec.2.4). With this modification, the rejection of Brownian bridge trajectories are decided faster and the efficiency of the algorithm is higher. Moreover, one should relax a little bit the assumption on the drift coefficient α .

Furthermore, we propose an unbiased algorithm to compute the derivatives (3) and (4). The idea combines Fournié et al. [5] formula and some generalization of Beskos et al. [2] rejection procedure.

The paper is organized as follows. We describe the algorithms in a general context in Section 2. Section 3 is devoted to a detailed presentation for the CIR model. We compare the efficiency of our algorithm with classical estimators in Section 4.

Acknowledgment: The authors would like to thank gratefully CA-CIB and Inria. This work started during an official collaboration between their teams. They are grateful to Inria Sophia Antipolis - Méditerranée “Nef” computation cluster for providing resources and support. They want also to thank Pierre Étoré for pointing out a mistake in a preliminary version of this work.

2 Unbiased Estimator

2.1 Beskos, Papaspiliopoulos and Roberts unbiased estimator

Here, we recall the main ideas developped in [3, 2] to exactly simulate the solution of one dimensional stochastic differential equations. Assume that the

process X^x solves the equation

$$X_T^x = x + \int_0^T \alpha(X_t^x) dt + W_T \quad (5)$$

(i.e. $\sigma \equiv 1$ in (1)). The main idea is a smart use of Girsanov Theorem:

$$\mathbb{E} \left[\Psi(X_T^x) \right] = \mathbb{E} \left[\Psi(B_T^x) \exp \left(\int_0^T \alpha(B_t^x) dB_t^x - \int_0^T \frac{\alpha^2(B_t^x)}{2} dt \right) \right]$$

where $(B_t^x)_{t \geq 0}$ is a one dimensional Brownian motion with $B_0^x = x$. The dimension allows one to transform the stochastic integral:

$$\int_0^T \alpha(B_t^x) dB_t^x = A(B_T^x) - A(B_0^x) - \int_0^T \frac{\alpha'(B_t^x)}{2} dt,$$

where $A(x) = \int_0^x \alpha(y) dy$. Then, one obtains

$$\mathbb{E} \left[\Psi(X_T^x) \right] = \mathbb{E} \left[\Psi(B_T^x) \exp \left(A(B_T^x) - A(B_0^x) - \int_0^T \frac{(\alpha^2 + \alpha')}{2} (B_t^x) dt \right) \right]. \quad (6)$$

Next, we replace in (6) the Brownian motion $(B_t^x, 0 \leq t \leq T)$ by a Brownian bridge $(\tilde{B}_t^x, 0 \leq t \leq T)$, where the final value \tilde{B}_T^x has the distribution

$$\mathbb{P}(\tilde{B}_T^x \in d\theta) = C \exp \left(-\frac{(\theta - x)^2}{2T} + \int_0^\theta \alpha(y) dy \right) d\theta. \quad (7)$$

Then, denote

$$\varphi(y) = \frac{\alpha^2(y) + \alpha'(y)}{2}, \quad (8)$$

one has

$$\mathbb{E} [\Psi(X_T^x)] = \tilde{C} \mathbb{E} \left[\Psi(\tilde{B}_T^x) \exp \left(- \int_0^T \varphi(\tilde{B}_t^x) dt \right) \right]. \quad (9)$$

If we moreover assume that φ takes value in a compact set, say $0 \leq \varphi(y) \leq K$, one can exactly simulate the diffusion X^x with a rejection procedure. Namely, one simulates a path of the Brownian bridge \tilde{B}^x and accept it with probability $\exp \left(- \int_0^T \varphi(\tilde{B}_t^x) dt \right)$. To do it, one simulates a Poisson process (independent of \tilde{B}^x) of unit intensity on $[0, T] \times [0, K]$ and accepts the Brownian bridge path if and only if there is no point of the Poisson process in the hypograph $D(\omega)$ of $\varphi(\tilde{B}_t^x)$

$$D(\omega) = \left\{ (t, y) \in [0, T] \times [0, K], y \leq \varphi(\tilde{B}_t^x) \right\}. \quad (10)$$

It is easy to verify that the probability to accept the path is $\exp \left(- \int_0^T \varphi(\tilde{B}_t^x) dt \right)$. Furthermore, we only need to know the value of the Brownian bridge at a finite number of times $0 < t_1 < \dots < t_n \leq T$, the abscissas of the points of the Poisson process. So, we have

$$\mathbb{E} [\Psi(X_T^x)] = \mathbb{E} \left[\Psi(\tilde{B}_T^x) \middle| N \cap D(\omega) = \emptyset \right], \quad (11)$$

where N is a Poisson process with unit intensity on $[0, T] \times [0, K]$, independent of $(\tilde{B}_t^x, 0 \leq t \leq T)$.

Remark 1. We have written this short presentation under the assumption $0 \leq \varphi \leq K$. It should be easily generalized to the cases where:

1. φ is bounded, but not necessary nonnegative. In this case, we only have to replace in (9) the function φ by $\varphi - \inf_{\mathbb{R}} \varphi$ and the constant \tilde{C} by $\tilde{C} \exp(-T \inf_{\mathbb{R}} \varphi)$.
2. φ has no finite global upper bound, but has an upper bound in $+\infty$ or $-\infty$. For instance, $\limsup_{y \rightarrow -\infty} \varphi(y) = +\infty$ and $\limsup_{y \rightarrow +\infty} \varphi(y) < \infty$. Here, we only have to first simulate the infimum $m(\omega)$ of \tilde{B}^x on $[0, T]$ and the time $t_m(\omega)$ at which it is reached. Then, we simulate a Poisson process on $[0, T] \times [0, \tilde{K}(\omega)]$ with $\tilde{K}(\omega) = \sup_{y \geq m(\omega)} \varphi(y)$ (see [2]).

Williams decomposition of Brownian paths [9] gives the conditional law $(\tilde{B}_t^x, 0 \leq t \leq T | m(\omega), t_m(\omega))$: conditionally to m and t_m , the processes $(\tilde{B}_{t_m+t}^x - m, 0 \leq t \leq T - t_m)$ and $(\tilde{B}_{t_m-t}^x - m, 0 \leq t \leq t_m)$ are two independent Bessel bridges processes of dimension 3. Such a process is simple to exactly simulate at a finite number of times.

2.2 Unbiased estimator of the first derivative (Delta)

In this section, we present our main results. We generalyse the unbiased algorithm introduced by Beskos et al. [2] to approximate the sensitivities $\frac{d}{dx} \mathbb{E}^x[\Psi(X_T)]$ with an unbiased estimator.

Proposition 1. *Let $(X_t^x, 0 \leq t \leq T)$ be the solution of (5), starting from x , and Ψ a measurable function. Assume that $\forall y \in \mathbb{R}$, we have $-\hat{K} \leq \alpha'(y) \leq 0$ and $0 \leq \alpha^2(y) + \alpha'(y) \leq 2K$. Then, an unbiased Monte Carlo procedure to evaluate $\frac{d}{dx} \mathbb{E} \Psi(X_T^x)$ is available*

$$\begin{aligned} \frac{d}{dx} \mathbb{E} \Psi(X_T^x) = & -\mathbb{E} \left[\frac{x \Psi(\tilde{B}_T^x)}{T} \middle| N \cap D = \emptyset \right] \\ & + \mathbb{E} \left[\frac{\Psi(\tilde{B}_T^x)}{T} \left(\tilde{B}_T^x - T \alpha(\tilde{B}_{U_2 T}^x) \right) \mathbb{1}_{\hat{N} \cap \hat{D} = \emptyset} \middle| N \cap D = \emptyset \right] \\ & - \mathbb{E} \left[\Psi(\tilde{B}_T^x) \left(\tilde{B}_{U_1 T}^x - U_1 T \alpha(\tilde{B}_{U_1 U_2 T}^x) \right) \alpha'(\tilde{B}_{U_1 T}^x) \mathbb{1}_{\hat{N} \cap \hat{D}^1 = \emptyset} \middle| N \cap D = \emptyset \right], \end{aligned}$$

where:

- $\varphi = (\alpha^2 + \alpha')/2$;
- $(\tilde{B}_t^x, 0 \leq t \leq T)$ is a Brownian bridge with \tilde{B}_T^x given by (7);
- D is the hypograph of $\varphi(\tilde{B}_t^x)$ (see (10));
- \hat{D} is the hypograph of $-\alpha'(\tilde{B}_t^x)$ and $\hat{D}_1 = \hat{D} \cap ([0, U_1 T] \times \mathbb{R}_+)$;
- N and \hat{N} are two independent Poisson processes with unit intensity on $[0, T] \times [0, K]$ and $[0, T] \times [0, \hat{K}]$, (and independent of \tilde{B}^x);
- U_1 and U_2 are two independent random variables with uniform distribution on $[0, 1]$ (and independent of \tilde{B}^x , N and \hat{N}).

We first recall basic results on Malliavin calculus (see Fournié et al. [5]) useful to detail our algorithm. The process $(X_t^x, t \geq 0)$ is the unique solution of (5) with $X_0^x = x$. We denote by $(Y_t^x, t \geq 0)$ the associated first variation process

$$Y_t^x := \frac{d}{dx} X_t^x.$$

It solves the linear SDE

$$\begin{aligned} dY_t^x &= Y_t^x \alpha'(X_t^x) dt \\ Y_0^x &= 1. \end{aligned}$$

The solution is

$$Y_t^x = \exp \left(\int_0^t \alpha'(X_s^x) ds \right). \quad (12)$$

Furthermore, it is known that the Malliavin derivative $D_t X_T^x$ satisfies

$$\begin{aligned} dD_t X_s^x &= D_t X_s^x \alpha'(X_s^x) ds \\ D_t X_t^x &= 1. \end{aligned} \quad (13)$$

We deduce that Y^x and $D_t X^x$ are linked by the identity

$$D_t X_T^x = \frac{Y_T^x}{Y_t^x}. \quad (14)$$

We deduce

$$Y_T^x = Y_t^x D_t X_T^x = \int_0^T a(t) Y_t^x D_t X_T^x dt,$$

where a is any L^2 function such that $\int_0^T a(t) dt = 1$. For instance, we use in this paper $a(t) \equiv \frac{1}{T}$.

Following Fournié et al. [5], and using classical results on Malliavin calculus (integration by parts formula, see [8]), we obtain

$$\begin{aligned} \frac{d}{dx} \mathbb{E} \Psi(X_T^x) &= \mathbb{E} [\Psi'(X_T^x) Y_T^x] \\ &= \frac{1}{T} \mathbb{E} \left[\int_0^T \Psi'(X_T^x) D_t(X_T^x) Y_t^x dt \right] = \frac{1}{T} \mathbb{E} \left[\int_0^T D_t(\Psi(X_T^x)) Y_t^x dt \right] \\ &= \frac{1}{T} \mathbb{E} [\Psi(X_T^x) \delta(Y_T^x)] \\ &= \frac{1}{T} \mathbb{E} \left[\Psi(X_T^x) \int_0^T Y_t^x dW_t \right]. \end{aligned} \quad (15)$$

Remark 2. Even if we have used the notation Ψ' in the sketch of the proof of the result, the relation remains true if Ψ is not a smooth function.

After this short remind on Malliavin calculus theory, we now prove Proposition 1.

Proof of Proposition 1. We use the one dimension setting to remove the stochastic integral in (15)

$$\begin{aligned} \int_0^T Y_t^x dW_t &= W_T Y_T^x - W_0 Y_0^x - \int_0^T W_t dY_t^x \\ &= W_T Y_T^x - W_0 Y_0^x - \int_0^T W_t Y_t^x \alpha'(X_t^x) dt. \end{aligned} \quad (16)$$

The evaluation of the integral in the last term would introduce a bias. To avoid it, one uses a classical identity. Namely, consider a stochastic process $(\gamma_t, 0 \leq t \leq T)$, we have

$$\int_0^T \gamma_t dt = T \bar{\mathbb{E}}(\gamma_{UT}) \quad (17)$$

where U is random variable with uniform distribution on $[0, 1]$, independent of γ and $\bar{\mathbb{E}}$ denotes the expectation with respect to U . The drawback of the last expression is the increase of the variance. See [7] for a discussion on this topic. Using this property and (12), we obtain

$$\begin{aligned} \frac{d}{dx} \mathbb{E} \Psi(X_T^x) = \mathbb{E} \left[\frac{\Psi(X_T^x)}{T} \left(W_T \exp \int_0^T \alpha'(X_s^x) ds - W_0 \right. \right. \\ \left. \left. - T W_{U_1 T} \alpha'(X_{U_1 T}^x) \exp \int_0^{U_1 T} \alpha'(X_s^x) ds \right) \right], \end{aligned}$$

where U_1 is a random variable independent of $(X_t^x, t \in [0, T])$ with uniform law on $[0, 1]$. As in Section 2.1, we finally apply Girsanov Theorem

$$\begin{aligned} \frac{d}{dx} \mathbb{E} \Psi(X_T^x) = \tilde{C} \mathbb{E} \left[\frac{\Psi(\tilde{B}_T^x)}{T} \exp \left(-\frac{1}{2} \int_0^T \alpha^2(\tilde{B}_s^x) + \alpha'(\tilde{B}_s^x) ds \right) \right. \\ \times \left(\left(\tilde{B}_T^x - \int_0^T \alpha(\tilde{B}_t^x) dt \right) \exp \int_0^T \alpha'(\tilde{B}_s^x) ds - x \right. \\ \left. \left. - T \left(\tilde{B}_{U_1 T}^x - \int_0^{U_1 T} \alpha(\tilde{B}_s^x) ds \right) \alpha'(\tilde{B}_{U_1 T}^x) \exp \int_0^{U_1 T} \alpha'(\tilde{B}_s^x) ds \right) \right], \end{aligned}$$

where $(\tilde{B}_t^x, 0 \leq t \leq T)$ is a Brownian bridge with final distribution given by (7) and $U_1 \sim \mathcal{U}(0, 1)$ is independent of \tilde{B}^x . We use the same rejection procedure as in Section 2.1 to obtain

$$\begin{aligned} \frac{d}{dx} \mathbb{E} \Psi(X_T^x) = \mathbb{E} \left[\frac{\Psi(\tilde{B}_T^x)}{T} \times \left((\tilde{B}_T^x - \int_0^T \alpha(\tilde{B}_t^x) dt) \exp \int_0^T \alpha'(\tilde{B}_s^x) ds - x \right. \right. \\ \left. \left. - T \left(\tilde{B}_{U_1 T}^x - \int_0^{U_1 T} \alpha(\tilde{B}_s^x) ds \right) \alpha'(\tilde{B}_{U_1 T}^x) \exp \int_0^{U_1 T} \alpha'(\tilde{B}_s^x) ds \right) \middle| N \cap D(\omega) = \emptyset \right]. \end{aligned}$$

$$\begin{aligned} \frac{d}{dx} \mathbb{E} \Psi(X_T^x) = -\mathbb{E} \left[\frac{x \Psi(\tilde{B}_T^x)}{T} \middle| N \cap D(\omega) = \emptyset \right] \\ + \mathbb{E} \left[\frac{\Psi(\tilde{B}_T^x)}{T} \left(\tilde{B}_T^x - T \alpha(\tilde{B}_{U_2 T}^x) \right) \exp \left(\int_0^T \alpha'(\tilde{B}_s^x) ds \right) \middle| N \cap D(\omega) = \emptyset \right] \\ - \mathbb{E} \left[\Psi(\tilde{B}_T^x) \left(\tilde{B}_{U_1 T}^x - U_1 T \alpha(\tilde{B}_{U_1 U_2 T}^x) \right) \alpha'(\tilde{B}_{U_1 T}^x) \right. \\ \left. \exp \left(\int_0^{U_1 T} \alpha'(\tilde{B}_s^x) ds \right) \middle| N \cap D(\omega) = \emptyset \right], \end{aligned}$$

where U_2 is a random variable with uniform distribution on $[0, 1]$, independent of \tilde{B}^x , N and U_1 .

It remains to remark that one again interprets the term $\exp\left(\int_0^T \alpha'(\tilde{B}_s^x) ds\right)$ as the probability for a Poisson process to have no point in a domain. More precisely, we consider a Poisson process \hat{N} with unit intensity on $[0, T] \times [0, \hat{K}]$ (where $\hat{K} = -\inf_{\mathbb{R}} \alpha'$), independent of \tilde{B}^x , N , U_1 and U_2 . We denote by \hat{D} the hypograph of $-\alpha'$

$$\hat{D}(\omega) = \left\{ (t, y) \in [0, T] \times \mathbb{R}^+, y \leq -\alpha'(\tilde{B}_t^x) \right\}$$

and by \hat{D}^1 its restriction to $[0, U_1 T] \times \mathbb{R}^+$. We finally have the unbiased estimator

$$\begin{aligned} \frac{d}{dx} \mathbb{E} \Psi(X_T^x) &= -\mathbb{E} \left[\frac{x \Psi(\tilde{B}_T^x)}{T} \middle| N \cap D(\omega) = \emptyset \right] \\ &\quad + \mathbb{E} \left[\frac{\Psi(\tilde{B}_T^x)}{T} \left(\tilde{B}_T^x - T \alpha(\tilde{B}_{U_2 T}^x) \right) \mathbb{1}_{\hat{N} \cap \hat{D} = \emptyset} \middle| N \cap D(\omega) = \emptyset \right] \\ &\quad - \mathbb{E} \left[\Psi(\tilde{B}_T^x) \left(\tilde{B}_{U_1 T}^x - U_1 T \alpha(\tilde{B}_{U_1 U_2 T}^x) \right) \alpha'(\tilde{B}_{U_1 T}^x) \mathbb{1}_{\hat{N} \cap \hat{D}^1 = \emptyset} \middle| N \cap D(\omega) = \emptyset \right]. \end{aligned} \tag{18}$$

□

Remark 3. Similarly to Remark 1, we can generalise the previous estimator to function φ with a global lower bound and an upper bound only in one side.

Furthermore, the same extension should be obtained if $-\alpha'$ has a global lower bound. In this case, we replace $-\alpha'$ by $-\alpha' + \sup_{\mathbb{R}}(\alpha')$ in the definition of \hat{K} , \hat{D} and \hat{D}^1 . We also replace $\mathbb{1}_{\hat{N} \cap \hat{D} = \emptyset}$ by $\exp(T \sup_{\mathbb{R}}(\alpha')) \mathbb{1}_{\hat{N} \cap \hat{D} = \emptyset}$ and $\mathbb{1}_{\hat{N} \cap \hat{D}^1 = \emptyset}$ by $\exp(U_1 T \sup_{\mathbb{R}}(\alpha')) \mathbb{1}_{\hat{N} \cap \hat{D}^1 = \emptyset}$.

Our unbiased estimator can be extended if $-\alpha'$ has only a local upper bound in the same side as φ (i.e. $\limsup_{y \rightarrow +\infty} \varphi(y)$ and $\limsup_{y \rightarrow +\infty} (-\alpha'(y))$ are both finite or $\limsup_{y \rightarrow -\infty} \varphi(y)$ and $\limsup_{y \rightarrow -\infty} (-\alpha'(y))$ are both finite).

2.3 Unbiased estimator of the second derivative (Gamma)

In this part, we detail an unbiased estimator of the second derivative $\frac{d^2}{dx^2} \mathbb{E} \Psi(X_T^x)$. We denote by Z_t^x the second variation process associated to X_t^x

$$Z_t^x = \frac{d^2}{dx^2} X_t^x.$$

It satisfies the linear stochastic differential equation

$$Z_T^x = \int_0^T \alpha''(X_s^x) (Y_s^x)^2 + \alpha'(X_s^x) Z_s^x ds.$$

The solution is

$$Z_T^x = Y_T^x \int_0^T \alpha''(X_s^x) Y_s^x ds. \tag{19}$$

We also need the Malliavin derivative of the first variation process Y^x . It satisfies

$$D_t Y_T^x = \int_0^T \alpha''(X_s^x) Y_s^x D_t X_s^x + \alpha'(X_s^x) D_t Y_s^x ds$$

The solution is

$$D_t Y_T^x = \frac{Y_T^x}{Y_t^x} \int_t^T \alpha''(X_s^x) Y_s^x ds. \quad (20)$$

As in the previous section, we present the computation under the assumption that Ψ is smooth. However, the final result remains true even if Ψ is only assumed to be measurable and bounded (see [5] for more details). Using (15), we formally derive with respect to x and obtain

$$\frac{d^2}{dx^2} \mathbb{E} \Psi(X_T^x) = \underbrace{\mathbb{E} \left[\frac{\Psi'(X_T^x)}{T} Y_T^x \int_0^T Y_t^x dW_t \right]}_{\Gamma_1(x)} + \underbrace{\mathbb{E} \left[\frac{\Psi(X_T^x)}{T} \int_0^T Z_t^x dW_t \right]}_{\Gamma_2(x)}.$$

The main steps to obtain a tractable unbiased expression of Γ_2 are identical to the ideas used in Section 2.2. We use the one dimensional setting to remove the stochastic integral and (20) to obtain

$$\begin{aligned} \Gamma_2(x) = \mathbb{E} \left[\frac{\Psi(X_T^x)}{T} \left(W_T Y_T^x \int_0^T \alpha''(X_t^x) Y_t^x dt - \int_0^T W_t (Y_t^x)^2 \alpha''(X_t^x) dt \right. \right. \\ \left. \left. - \int_0^T \int_0^t W_t \alpha'(X_t^x) \alpha''(X_u^x) Y_u^x Y_t^x du dt \right) \right] \quad (21) \end{aligned}$$

To simplify Γ_1 , we apply the Malliavin integration by part formula and (14)

$$\begin{aligned} \Gamma_1(x) &= \frac{1}{T^2} \mathbb{E} \left[\int_0^T D_t(\Psi(X_T^x)) Y_t^x \int_0^T Y_s^x dW_s dt \right] \\ &= \frac{1}{T^2} \mathbb{E} \left[\Psi(X_T^x) \delta \left(Y_T^x \int_0^T Y_s^x dW_s \right) \right]. \end{aligned}$$

Finally, we have to make explicit the divergence operator. We apply [8, Prop. 1.3.3] to obtain

$$\begin{aligned} \delta \left(Y_t^x \int_0^T Y_s^x dW_s \right) &= \int_0^T Y_s^x dW_s \delta(Y_t^x) - \int_0^T D_t \left(\int_0^T Y_s^x dW_s \right) Y_t^x dt \\ \text{and } D_t \left(\int_0^T Y_s^x dW_s \right) &= Y_t^x + \int_t^T D_t Y_s^x dW_s. \end{aligned}$$

We again simplify the stochastic integral

$$\begin{aligned} \int_t^T D_t Y_s^x dW_s &= (D_t Y_T^x) W_T - \int_t^T W_s \alpha''(X_s^x) Y_s^x \frac{Y_s^x}{Y_t^x} ds \\ &\quad - \int_t^T W_s \frac{\alpha'(X_s^x) Y_s^x}{Y_t^x} \int_t^s \alpha''(X_u^x) Y_u^x du ds. \end{aligned}$$

Finally, denoting U_1 , U_2 and U_3 three uniform independent random variables, independent of W and using (17), we obtain

$$\begin{aligned} \frac{d^2}{dx^2} \mathbb{E} \Psi(X_T^x) = \mathbb{E} \left[\Psi(X_T^x) \left(\frac{x^2}{T^2} - \frac{2x}{T^2} W_T Y_T^x + \frac{1}{T^2} (W_T)^2 (Y_T^x)^2 \right. \right. \\ \left. \left. + \frac{2x}{T} W_{U_1 T} \alpha'(X_{U_1 T}^x) Y_{U_1 T}^x \right. \right. \\ \left. \left. - \frac{1}{T} (Y_{U_1 T}^x)^2 + (U_1 - 1) W_{U_1 T} \alpha''(X_{U_1 T}^x) (Y_{U_1 T}^x)^2 \right. \right. \\ \left. \left. + W_{U_1 T} \alpha'(X_{U_1 T}^x) W_{U_2 T} \alpha'(X_{U_2 T}^x) Y_{U_1 T}^x Y_{U_2 T}^x \right. \right. \\ \left. \left. - \frac{2W_T}{T} W_{U_1 T} \alpha'(X_{U_1 T}^x) Y_T^x Y_{U_1 T}^x + W^x(T) (1 - U_1) \alpha''(X_{U_1 T}^x) Y_T^x Y_{U_1 T}^x \right. \right. \\ \left. \left. + U_1 T (U_1 U_2 - 1) W_{U_1 T} \alpha'(X_{U_1 T}^x) \alpha''(X_{U_1 U_2 T}^x) Y_{U_1 U_2 T}^x Y_{U_1 T}^x \right) \right]. \end{aligned}$$

Similarly to Sections 2.1 and 2.2, we apply Girsanov theorem and (12). We change in the previous expression

$$\begin{aligned} X_s^x &\rightarrow \tilde{B}_s^x \\ W_s &\rightarrow \tilde{B}_s^x - s\alpha(\tilde{B}_{U_s}^x). \end{aligned}$$

$$\begin{aligned}
\frac{d^2}{dx^2} \mathbb{E} \Psi(X_T^x) &= \mathbb{E} \left[\Psi(\tilde{B}_T^x) \left(\frac{x^2}{T^2} - \frac{2x}{T^2} (\tilde{B}_T^x - T\alpha(\tilde{B}_{U_3T}^x)) \exp \left(\int_0^T \alpha'(\tilde{B}_\theta^x) d\theta \right) \right. \right. \\
&\quad + \frac{1}{T^2} (\tilde{B}_T^x - T\alpha(\tilde{B}_{U_3T}^x)) (\tilde{B}_T^x - T\alpha(\tilde{B}_{U_4T}^x)) \exp \left(\int_0^T 2\alpha'(\tilde{B}_\theta^x) d\theta \right) \\
&\quad + \frac{2x}{T} (\tilde{B}_{U_1T}^x - U_1T\alpha(\tilde{B}_{U_1U_3T}^x)) \alpha'(\tilde{B}_{U_1T}^x) \exp \left(\int_0^{U_1T} \alpha'(\tilde{B}_\theta^x) d\theta \right) \\
&\quad \quad \quad - \frac{1}{T} \exp \left(\int_0^{U_1T} 2\alpha'(\tilde{B}_\theta^x) d\theta \right) \\
&\quad + (U_1 - 1) (\tilde{B}_{U_1T}^x - U_1T\alpha(\tilde{B}_{U_1U_3T}^x)) \alpha''(\tilde{B}_{U_1T}^x) \exp \left(\int_0^{U_1T} 2\alpha'(\tilde{B}_\theta^x) d\theta \right) \\
&\quad + (\tilde{B}_{U_1T}^x - U_1T\alpha(\tilde{B}_{U_1U_3T}^x)) \alpha'(\tilde{B}_{U_1T}^x) (\tilde{B}_{U_2T}^x - U_2T\alpha(\tilde{B}_{U_2U_4T}^x)) \alpha'(\tilde{B}_{U_2T}^x) \\
&\quad \quad \quad \times \exp \left(\int_0^{U_1T} \alpha'(\tilde{B}_\theta^x) d\theta \right) \exp \left(\int_0^{U_2T} \alpha'(\tilde{B}_\theta^x) d\theta \right) \\
&\quad - \frac{2}{T} (\tilde{B}_T^x - T\alpha(\tilde{B}_{U_3T}^x)) (\tilde{B}_{U_1T}^x - U_1T\alpha(\tilde{B}_{U_1U_4T}^x)) \alpha'(\tilde{B}_{U_1T}^x) \\
&\quad \quad \quad \times \exp \left(\int_0^T \alpha'(\tilde{B}_\theta^x) d\theta \right) \exp \left(\int_0^{U_1T} \alpha'(\tilde{B}_\theta^x) d\theta \right) \\
&\quad \quad \quad + (\tilde{B}_T^x - T\alpha(\tilde{B}_{U_3T}^x)) (1 - U_1) \alpha''(\tilde{B}_{U_1T}^x) \\
&\quad \quad \quad \times \exp \left(\int_0^T \alpha'(\tilde{B}_\theta^x) d\theta \right) \exp \left(\int_0^{U_1T} \alpha'(\tilde{B}_\theta^x) d\theta \right) \\
&\quad + U_1T (U_1U_2 - 1) (\tilde{B}_{U_1T}^x - U_1T\alpha(\tilde{B}_{U_1U_3T}^x)) \alpha'(\tilde{B}_{U_1T}^x) \alpha''(\tilde{B}_{U_1U_2T}^x) \\
&\quad \quad \quad \exp \left(\int_0^{U_1U_2T} \alpha'(\tilde{B}_\theta^x) d\theta \right) \exp \left(\int_0^{U_2T} \alpha'(\tilde{B}_\theta^x) d\theta \right) \Big| N \cap D = \emptyset \Big].
\end{aligned}$$

To conclude, each term on the form $\exp(-\int_0^s \beta(\tilde{B}_\theta^x) d\theta)$ is replaced by $\mathbb{E} \mathbb{1}_{\{N^j \cap D^j = \emptyset\}}$ for appropriate Poisson processes N^j and hypograph D^j (similar terms are expressed in details p. 7).

2.4 Simulation of the Poisson Process

We have recalled in Section 2.1 the details of the algorithm developped in [2] to simulate exact paths of the solution of (5). The main point is the following. Consider a function φ with values in $[0, K]$, $\exp(-\int_0^T \varphi(\tilde{B}_\theta^x) d\theta)$ is the probability that $N \cap D = \emptyset$, where N is a Poisson process with unit intensity on $[0, T] \times [0, K]$ independent of \tilde{B}^x . The hypograph D of $\varphi(\tilde{B}_\theta^x)$ is defined by (10).

For the rejection procedure, we simulate the Poisson process $(t_1, y_1), \dots, (t_{n(\omega)}, y_{n(\omega)})$ and the Brownian bridge at the times $t_1, \dots, t_{n(\omega)}$. If there exists $j \in [1, n(\omega)]$ such that $y_j < \varphi(\tilde{B}_{t_j}^x)$, the Brownian bridge path is rejected.

In [2], the Poisson process is generated on $[0, T] \times [0, K]$. The result is $((t_1, y_1), \dots, (t_{n(\omega)}, y_{n(\omega)}))$. Then, the authors simulate the Brownian bridge at time $t_1, t_2, \dots, t_{n(\omega)}$ and evaluate the cardinal number of $N \cap D$. In the present paper, we propose two variants of the algorithm. For both variants, immediatly after the simulation of one point (t_j, y_j) , we simulate $\tilde{B}_{t_j}^x$. If $y_j < \varphi(\tilde{B}_{t_j}^x)$, we have to reject the Brownian bridge path. So, we do not need to simulate the full Poisson process N and stop immediatly the algorithm. There is two simple variants for the simulation of the Poisson process: first, by increasing times $(t_1 < t_2 < \dots < t_{n(\omega)})$. Second, by increasing ordinates $(y_1 < y_2 < \dots < y_{n(\omega)})$. This last variant aims to reject as fast as possible the Brownian bridge trajectory. Roughly speaking, smaller is the ordinate, higher is the probability to be below $\varphi(\tilde{B}^x)$. We numerically compare the efficiency of the both variants in Section 4.1.2.

2.5 A truncated algorithm

The increasing ordinates variant should start, even if we do not know an explicit upper bound K to $t \mapsto \varphi(\tilde{B}_t^x)$. We propose to extend the Beskos et al. algorithm to SDE with drift α , such that $\limsup_{y \rightarrow -\infty} \varphi(y) = \limsup_{y \rightarrow +\infty} \varphi(y) = \infty$. According to [2], $\varphi = (\alpha^2 + \alpha')/2$.

For any $L > 0$, we denote N^L a Poisson process with unit intensity on $[0, T] \times [0, L]$. Our truncated algorithm is stopped and we accept a path of the Brownian bridge if $N^{\tilde{K}(\omega)} \cap D = \emptyset$, where $\tilde{K}(\omega) \leq \sup_{\theta \in [0, T]} \{\varphi(\tilde{B}_\theta^x)\}$. Larger is \tilde{K} , smaller is the probability to wrongly accept a path, but slower is the algorithm. A reasonable choice of $\tilde{K}(\omega)$ is

$$\tilde{K}(\omega) \geq \max\{K, \varphi(\tilde{B}_T^x), \varphi(\inf_{0 \leq s \leq T} \tilde{B}_s^x)\},$$

where K is an a priori threshold. Our algorithm is no more unbiased. However, Proposition 2 gives an upper bound of the error in the approximation of (2).

2.6 Theoretical Control of the error

Proposition 2. *Let X_T^x solution of (5) and $X_T^{x,K}$ its approximation obtained by the truncated rejection procedure presented in Section 2.4. Precisely, the Brownian bridge path is accepted if there is no point of an independent Poisson process on $[0, T] \times [0, K]$ in the hypograph D of φ (given by (10)). Then:*

a.

$$\begin{aligned} & \left| \mathbb{E}\Psi(X_T^x) - \mathbb{E}\Psi(X_T^{x,K}) \right| \\ & \leq \sqrt{\mathbb{E}[\Psi^2(\tilde{B}_T^x)]} \left(\frac{\mathbb{P}(\sup_{0 \leq \theta \leq T} \varphi(\tilde{B}_\theta^x) > K)}{p_K \sqrt{p_\infty}} + \frac{\sqrt{\mathbb{P}(\sup_{0 \leq \theta \leq T} \varphi(\tilde{B}_\theta^x) > K)}}{p_K} \right), \end{aligned} \tag{22}$$

where p_K denotes the probability to accept a Brownian bridge path with the truncated algorithm at level K ,

$$p_K = \mathbb{E} \left[\exp \left(- \int_0^T K \wedge \varphi(\tilde{B}_\theta^x) d\theta \right) \right] \quad (23)$$

and p_∞ is given by

$$p_\infty = \mathbb{E} \left[\exp \left(- \int_0^T \varphi(\tilde{B}_\theta^x) d\theta \right) \right].$$

b. If moreover Ψ is bounded,

$$\left| \mathbb{E}\Psi(X_T^x) - \mathbb{E}\Psi(X_T^{x,K}) \right| \leq \frac{2\|\Psi\|_\infty}{p_K} \mathbb{P} \left(\sup_{0 \leq \theta \leq T} \varphi(\tilde{B}_\theta^x) > K \right). \quad (24)$$

Remark 4. 1. If $\limsup_{y \rightarrow -\infty} \varphi(y) = \limsup_{y \rightarrow +\infty} \varphi(y) = +\infty$, for any Brownian bridge, the probability to wrongly accept the trajectory is positive. However, Proposition 2 gives a control of the error.

2. The result of Proposition 2 still holds true if we use the variant of the algorithm with the simulation of the minimum of the Brownian bridge (see point 2) of Remark 1 and [2]). Numerical results for this variant are given in Section 4.1.2.

3. If we have a control of the asymptotic behavior of φ (e.g. a polynomial growth at infinity), we deduce that the error of truncation decreases exponentially fast to 0 with K .

Proof. We denote by N^K a Poisson process on $[0, T] \times [0, K]$ and by N a Poisson process on $[0, T] \times \mathbb{R}_+$. Thanks to (11), we have

$$\begin{aligned} \mathbb{E}\Psi(X_T^x) &= \mathbb{E} \left[\Psi(\tilde{B}_T^x) \middle| N \cap D(\omega) = \emptyset \right] \\ &= \frac{\mathbb{E} \left[\Psi(\tilde{B}_T^x) \exp \left(- \int_0^T \varphi(\tilde{B}_\theta^x) d\theta \right) \right]}{\mathbb{E} \left[\exp \left(- \int_0^T \varphi(\tilde{B}_\theta^x) d\theta \right) \right]} \\ \mathbb{E}\Psi(X_T^{x,K}) &= \mathbb{E} \left[\Psi(\tilde{B}_T^x) \middle| N^K \cap D(\omega) = \emptyset \right], \\ &= \frac{\mathbb{E} \left[\Psi(\tilde{B}_T^x) \exp \left(- \int_0^T K \wedge \varphi(\tilde{B}_\theta^x) d\theta \right) \right]}{\mathbb{E} \left[\exp \left(- \int_0^T K \wedge \varphi(\tilde{B}_\theta^x) d\theta \right) \right]}. \end{aligned}$$

We denote by p_K (resp. p_∞) the probability to accept a Brownian bridge path with the truncated algorithm at level K (resp. with the exact algorithm).

$$p_K = \mathbb{E} \left[\exp \left(- \int_0^T K \wedge \varphi(\tilde{B}_\theta^x) d\theta \right) \right], \quad (25)$$

$$p_\infty = \mathbb{E} \left[\exp \left(- \int_0^T \varphi(\tilde{B}_\theta^x) d\theta \right) \right]. \quad (26)$$

Thus, a control of the error is

$$\begin{aligned} \text{err}_K &= \left| \mathbb{E} \Psi(X_T^x) - \mathbb{E} \Psi(X_T^{x,K}) \right| \\ &\leq \left| \frac{1}{p_\infty} - \frac{1}{p_K} \right| \mathbb{E} \left[\left| \Psi(\tilde{B}_T^x) \right| \exp \left(- \int_0^T \varphi(\tilde{B}_\theta^x) d\theta \right) \right] \\ &\quad + \frac{1}{p_K} \mathbb{E} \left[\left| \Psi(\tilde{B}_T^x) \right| \left(\exp \left(- \int_0^T K \wedge \varphi(\tilde{B}_\theta^x) d\theta \right) - \exp \left(- \int_0^T \varphi(\tilde{B}_\theta^x) d\theta \right) \right) \right]. \end{aligned}$$

We apply Cauchy-Schwarz inequality and use that $x^2 \leq x$ for $0 \leq x \leq 1$

$$\begin{aligned} \text{err}_K &\leq \frac{p_K - p_\infty}{p_K p_\infty} \sqrt{\mathbb{E} \left[\Psi^2(\tilde{B}_T^x) \right]} \sqrt{p_\infty} \\ &\quad + \frac{1}{p_K} \sqrt{\mathbb{E} \left[\Psi^2(\tilde{B}_T^x) \right]} \sqrt{\mathbb{E} \left[\exp \left(- \int_0^T K \wedge \varphi(\tilde{B}_\theta^x) d\theta \right) - \exp \left(- \int_0^T \varphi(\tilde{B}_\theta^x) d\theta \right) \right]} \\ &\leq \sqrt{\mathbb{E} \left[\Psi^2(\tilde{B}_T^x) \right]} \left(\frac{p_K - p_\infty}{p_K \sqrt{p_\infty}} + \frac{\sqrt{p_K - p_\infty}}{p_K} \right). \end{aligned}$$

We finally observe that

$$p_K - p_\infty \leq \mathbb{P} \left(\sup_{0 \leq \theta \leq T} \varphi(\tilde{B}_\theta^x) > K \right).$$

The proof under the assumption that Ψ is bounded is very similar, except we do not need to apply Cauchy-Schwarz inequality. It is left to the reader. \square

3 The detailed algorithm for the CIR Model

This section is devoted to the extension of our algorithm to the simulation of the Cox Ingersoll Ross (CIR) process, a popular model in finance (for short rates or volatility for stochastic volatility model on asset, etc.) This process satisfies

$$V_T = V_0 + \int_0^T \kappa (V_\infty - V_t) dt + \varepsilon \int_0^T \sqrt{V_t} dW_t \quad (27)$$

where κ , V_∞ and ε are fixed constants. Usually, the parameter $d = \frac{4\kappa V_\infty}{\varepsilon^2}$ is called the degree of the CIR process. It is known that $\mathbb{P}(\inf_{\theta \in [0, T]} V_\theta > 0) = 1$ iff $d \geq 2$ (see e.g. [1]). We assume it is fulfilled. We apply the Lamperti transform to the process V , that is we set

$$X_t = \frac{2\sqrt{V_t}}{\varepsilon} =: \eta(V_t).$$

The process X satisfies the SDE

$$\begin{aligned} dX_t &= \eta'(V_t) dV_t + \frac{1}{2} \eta''(V_t) d\langle V \rangle_t \\ &= \frac{1}{\varepsilon \sqrt{V_t}} \left(\kappa (V_\infty - V_t) dt + \varepsilon \sqrt{V_t} dW_t \right) - \frac{\varepsilon^2 V_t}{4\varepsilon V_t^{3/2}} dt \\ &= \left(\frac{1}{X_t} \left(\frac{2\kappa V_\infty}{\varepsilon^2} - \frac{1}{2} \right) - \frac{\kappa X_t}{2} \right) dt + dW_t. \end{aligned} \quad (28)$$

It is an SDE of type (5) with

$$\alpha(y) = \frac{1}{y} \left(\frac{2\kappa V_\infty}{\varepsilon^2} - \frac{1}{2} \right) - \frac{\kappa y}{2} \text{ for } y > 0.$$

The associated function φ defined by (8) is

$$\varphi(y) = \left(\left(\frac{2\kappa V_\infty}{\varepsilon^2} - 1 \right)^2 - \frac{1}{4} \right) \frac{1}{2y^2} + \frac{\kappa^2}{8} y^2 - \frac{\kappa^2 V_\infty}{\varepsilon^2}.$$

The function φ is bounded below on $(0, +\infty)$ iff

$$\left(\frac{2\kappa V_\infty}{\varepsilon^2} - 1 \right)^2 \geq \frac{1}{4}$$

or equivalently that the degree d of the CIR satisfies $d \in (0, 1] \cup [3, \infty)$. In this paper, we assume $d \geq 3$.

Remark 5. In Section 2, the drift α is defined on \mathbb{R} . However, a classical Feller test proves that the process X^x , the solution of (28) starting from $x > 0$, never hits 0 almost surely. Formally, if we put $\alpha(y) = \varphi(y) = +\infty$ for all $y \leq 0$, the Brownian bridge paths \tilde{B} taking values in \mathbb{R}_- are almost surely rejected.

3.1 Final Value

In the first step, we generate the final value \tilde{B}_T^x according to (7). Its density is

$$h(y) = Ry^c \exp \left(-\frac{(y - \hat{x})^2}{2\sigma^2} \right) \mathbb{1}_{y \geq 0}$$

with:

$$c = \frac{2\kappa V_\infty}{\varepsilon^2} - \frac{1}{2}, \quad \hat{x} = 2\sigma^2 \frac{x}{2T}, \quad x = \frac{2}{\varepsilon} \sqrt{V_0}, \quad \sigma^2 = \frac{1}{\frac{\kappa}{2} + \frac{1}{T}}$$

and R is a normalization. Setting $\bar{x} = \frac{\hat{x} + \sqrt{\hat{x}^2 + 4c\sigma^2}}{2}$, there exists $C > 0$ such that

$$\forall y, \quad h(y) \leq C \exp \left(-\frac{(y - \bar{x})^2}{2\sigma^2} \right),$$

and we use the classical rejection procedure for random variables.

3.2 Simulation of the minimum

The second step consists in generating the random variables (m, t_m) , where

$$m = \inf_{0 \leq t \leq T} \left\{ \tilde{B}_t^x \mid \tilde{B}_0 = x, \tilde{B}_T^x = Y \right\} \quad \tilde{B}_{t_m}^x = m$$

This law is known (see for instance Karatzas-Shreve [6, p. 102])

$$\mathbb{P} \left[m \in d\alpha, t_m \in ds \mid \tilde{B}_T^x = Y \right] = \frac{\alpha(\alpha - Y)}{\sqrt{s^3(T-s)^3}} \exp \left(-\frac{\alpha^2}{2s} - \frac{(\alpha - Y)^2}{2(T-s)} \right) d\alpha ds.$$

In Beskos et al. [2, Prop. 2], the detailed random variables used to simulate (m, t_m) are given: the authors only need to simulate uniform, exponential and Inverse Gaussian distributions (see Devroye [4, p.149] for an efficient way to simulate Inverse Gaussian distributions).

3.3 Simulation of the Poisson process

We apply the method detailed in Section 2.4. We generate $z_1 \sim \mathcal{E}(T)$, $t_1 \sim \mathcal{U}(0, T)$, $\tilde{B}_{t_1}^x$ conditioned by $\tilde{B}_0^x, \tilde{B}_T^x, m, t_m$. If $\varphi(\tilde{B}_{t_1}^x) > z_1$, we reject the trajectory. Else, we generate $z_2 - z_1 \sim \mathcal{E}(T)$, $t_2 \sim \mathcal{U}(0, T)$, $\tilde{B}_{t_2}^x$ conditioned by $\tilde{B}_0^x, \tilde{B}_{t_1}^x, \tilde{B}_T^x, m, t_m$. If $\varphi(\tilde{B}_{t_2}^x) > z_2$, we reject the trajectory, etc.

3.4 Stopping condition

In this example, $\sup_{y \geq m(\omega)} \varphi(y) = +\infty$. So, we use the truncated algorithm presented in Section 2.5. We simulate the Poisson process on $[0, T] \times [0, \tilde{K}(\omega)]$ with

$$\tilde{K}(\omega) \geq \max\{K, \varphi(\tilde{B}_T^x), \varphi(m)\}, \quad (29)$$

where K is a fixed a priori threshold.

4 Numerical Results

In this Section, we present the numerical results. We first apply the algorithm to an academic example related to Ornstein-Uhlenbeck process (Section 4.1). The drift α is constructed such that its associated function φ satisfies $\limsup_{y \rightarrow \infty} \varphi(y) < \infty$. In Section 4.2, the drift α is constructed in such a way that the associated function φ satisfies $\limsup_{y \rightarrow -\infty} \varphi(y) = \limsup_{y \rightarrow \infty} \varphi(y) = \infty$. Finally, Section 4.3 is devoted to the CIR process (see Section 3), i.e. an example with a non Lipschitz continuous drift α .

We use the algorithms to approximate quantities (2), (3) and (4) for smooth and nonsmooth functions Ψ . We compare the efficiency of our algorithm to the use of a classical Euler scheme and finite difference approximation of the derivatives.

4.1 An academic example: a modified Ornstein Uhlenbeck

4.1.1 Definition

We introduce the process $(X_t^x, t \geq 0)$, solution of

$$dX_t^x = \left(-M \left(X_t^x + \frac{1}{2} \right) \mathbb{1}_{X_t^x \leq -1} + \frac{M}{2} (X_t^x)^2 \mathbb{1}_{-1 \leq X_t^x \leq 0} \right) dt + dW_t, \quad (30)$$

where $M \geq 1/2$ is a fixed parameter. The process X^x is solution of an SDE of type (5) with a drift $\alpha \in C^1(\mathbb{R})$. Its associated function φ is

$$\varphi(y) = \begin{cases} 0 & \text{if } y \geq 0 \\ \frac{M^2 y^4}{8} + \frac{M y}{2} & \text{if } -1 \leq y \leq 0 \\ \frac{M^2}{2} \left(y + \frac{1}{2} \right)^2 - \frac{M}{2} & \text{if } y \leq -1. \end{cases}$$

It satisfies

$$\lim_{y \rightarrow -\infty} \varphi(y) = +\infty \quad \text{and} \quad \lim_{y \rightarrow +\infty} \varphi(y) < \infty.$$

Then, SDE (30) satisfies the assumptions made in Section 2 and we are in position to apply our unbiased algorithm to approximate $\mathbb{E}(\Psi(X_T^x))$, $\frac{d}{dx}\mathbb{E}(\Psi(X_T^x))$ and $\frac{d^2}{dx^2}\mathbb{E}(\Psi(X_T^x))$ for general functions Ψ .

4.1.2 Algorithmic optimization of computation time

We have discussed in Section 2.4 two variants to simulate the Poisson process N used to reject (or accept) the Brownian bridge paths.

- **variant 1** by increasing times: a realization of N , say $\{(t_1, y_1), \dots, (t_{n(\omega)}, y_{n(\omega)})\}$, satisfies $t_1 < t_2 < \dots < t_{n(\omega)}$.
- **variant 2** by increasing ordinates: $\{(t_1, y_1), \dots, (t_{n(\omega)}, y_{n(\omega)})\}$ satisfies $y_1 < y_2 < \dots < y_{n(\omega)}$.

In this part, we compare the efficiency of the two variants. They only differ by the computation time used to accept a Brownian bridge path. Figure 1 represents the time of simulation as a function of the final time T . The size of the sample is $N_{MC} = 1e6$ and the parameters are $x = 0.04$, $M = 0.5$.

We observe that the times of simulation are very close for small values of T ; they both increase exponentially and, clearly, the rate is smaller for variant 2 than variant 1.

We then fix the final time $T = 1$ and change the parameter M in the drift α (see (30)). The times of simulation of a sample of size $N_{MC} = 1e6$ are given in Table. 1. Again, the variant 2 is faster than variant 1.

M	time (var. 1)	time (var. 2)	Ratio
1	7.79	7.74	0.99
10	31	14	2.21
100	254591	5148	49.4

Table 1: Comparison of the times (in sec.) of simulation for variant 1 (increasing times) and variant 2 (increasing ordinates). We simulate $N_{MC} = 1e6$ values of X_T ($x = 0$, $T = 1$, $M = 1, 10, 100$).

4.1.3 A comparison of approximations of sensitivities

The unbiased evaluation of the sensitivities $\frac{d}{dx}\mathbb{E}^x\Psi(X_T)$ and $\frac{d^2}{dx^2}\mathbb{E}^x\Psi(X_T)$ are the main new results of the paper. They are themselves interesting theoretical results. However, we aim to compare their efficiency to classical numerical methods.

Our unbiased estimator It is fully presented in Section 2. We apply a classical Monte Carlo procedure to evaluate the expressions (11), (18) and the expression p.10 for the second derivative. We denote the Monte Carlo estimators by

$$\tilde{P}_\Psi(N_{MC}), \quad \tilde{\Delta}_\Psi(N_{MC}), \quad \tilde{\Gamma}_\Psi(N_{MC}).$$

There is a unique source of error: the statistical error. It is only related to the variance of the expressions we evaluate. In Table 2, we present the results for

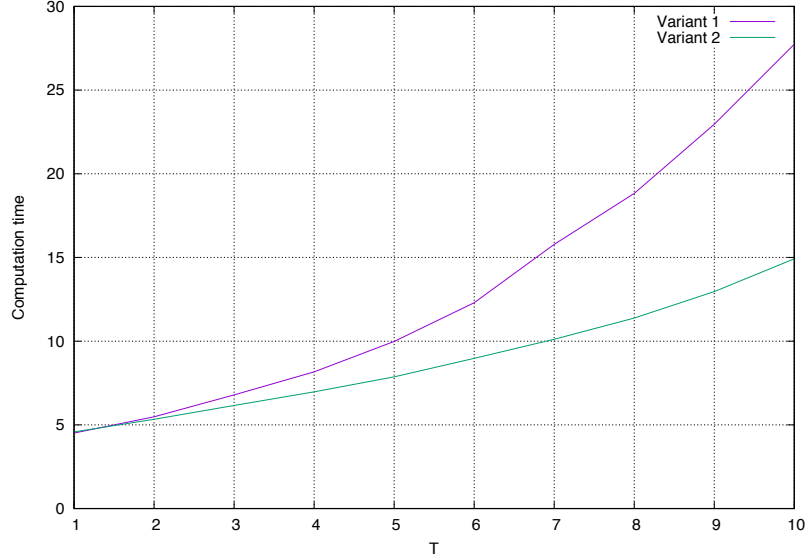


Figure 1: Comparison of the times of simulation for two methods to generate the Poisson process: variant 1 (increasing times) and variant 2 (increasing ordinate). Times of simulation (in seconds) are given in function of the final time T . The process X^x solves (30). The parameters are $M = 0.5$, $x = 0.04$ and $N_{MC} = 1e6$.

three functions Ψ , two are smooth and the last one is discontinuous. We put in brackets the estimated statistical standard deviation with a sample of size $N_{MC} = 2e10$.

Standard estimator using Euler scheme and finite difference approximation We simulate $X_T^{x,\delta,1}, \dots, X_T^{x,\delta,N_{MC}}$, N_{MC} independent realisations of the explicit Euler scheme (with time step δ) to approximate the solution X_T^x of (5). The derivatives are approximated with a finite difference scheme. That is, we simulate $X_T^{x-dx,\delta,1}, \dots, X_T^{x-dx,\delta,N_{MC}}$ and $X_T^{x+dx,\delta,1}, \dots, X_T^{x+dx,\delta,N_{MC}}$ and

use the estimators

$$\begin{aligned}
\hat{P}_\Psi(N_{\text{MC}}, \delta) &:= \frac{1}{N_{\text{MC}}} \sum_{k=1}^{N_{\text{MC}}} \Psi(X_T^{x, \delta, k}) \\
&\approx \mathbb{E}(\Psi(X_T^x)), \\
\hat{\Delta}_\Psi(N_{\text{MC}}, \delta, dx) &:= \frac{1}{2dx N_{\text{MC}}} \left(\sum_{k=1}^{N_{\text{MC}}} \Psi(X_T^{x+dx, \delta, k}) - \sum_{k=1}^{N_{\text{MC}}} \Psi(X_T^{x-dx, \delta, k}) \right) \\
&\approx \frac{d}{dx} \mathbb{E}(\Psi(X_T^x)), \\
\hat{\Gamma}_\Psi(N_{\text{MC}}, \delta, dx) &:= \frac{1}{(dx)^2 N_{\text{MC}}} \left(\sum_{k=1}^{N_{\text{MC}}} \Psi(X_T^{x+dx, \delta, k}) - 2 \sum_{k=1}^{N_{\text{MC}}} \Psi(X_T^{x, \delta, k}) \right. \\
&\quad \left. + \sum_{k=1}^{N_{\text{MC}}} \Psi(X_T^{x-dx, \delta, k}) \right) \\
&\approx \frac{d^2}{dx^2} \mathbb{E}(\Psi(X_T^x))
\end{aligned}$$

These approximations are also very simple to simulate and evaluate. We now have two sources of error:

- a bias due to the parameters δ and dx .
- the statistical error, related to the variance of the quantities we estimate with a Monte Carlo procedure.

In practice, we have to carefully choose N , δ and dx . The best choice is obtained if the bias is close to the statistical error. It is not easy to reach such a balance because we do not know the bias.

We have chosen two set of parameters, $N_{\text{MC}} = 1e9$, $\delta = 0.1$ and $dx = 0.4$ in Table 4 and $N_{\text{MC}} = 5e7$, $\delta = 0.005$ and $dx = 0.1$ in Table 3.

$\Psi(y)$	$\tilde{P}_\Psi(N_{\text{MC}})$	$\tilde{\Delta}_\Psi(N_{\text{MC}})$	$\tilde{\Gamma}_\Psi(N_{\text{MC}})$
y^2	0.900933 (9.0e-6)	0.301072 (2.5e-5)	1.57485 (5.6e-5)
$\exp(-y)$	1.40071 (1.1e-5)	-1.16071 (2.8e-5)	0.703935 (7.2e-5)
$\mathbb{1}_{y>x}$	0.492925 (3.5e-6)	-0.3854 (4.7e-6)	-0.0219749 (8.3e-6)

Table 2: Approximation for X^x solution of (30) obtained with our unbiased algorithms. $N_{\text{MC}} = 2e10$, $M = 0.5$, $x = 0.04$. The program run 9e4 seconds.

Conclusion To obtain an error of the same magnitude with our unbiased estimator, we have to use between $N_{\text{MC}} = 1e5$ and $N_{\text{MC}} = 1e6$ for the rough case (Table 3) and between $N_{\text{MC}} = 1e6$ and $N_{\text{MC}} = 1e7$ for the more precise case (Table 4). The size of the sample obviously depends on the function Ψ and the order of the derivative we approximate. Our algorithm is well adapted for the approximation of Δ_Ψ and Γ_Ψ .

$\Psi(y)$	$\hat{P}_\Psi(N_{\text{MC}}, \delta)$ $-P_\Psi$	$\hat{\Delta}_\Psi(N_{\text{MC}}, \delta, dx)$ $-\Delta_\Psi$	$\hat{\Gamma}_\Psi(N_{\text{MC}}, \delta, dx)$ $-\Gamma_\Psi$
y^2	8.8e-3 (4.1e-5)	5.0e-3 (1.1e-4)	1.1e-3 (1.1e-3)
$\exp(-y)$	1.5e-2 (4.9e-5)	-2e-2 (1.3e-4)	7.0e-3 (1.2e-3)
$\mathbb{1}_{y>x}$	-7.1e-5 (1.6e-5)	1.1e-2 (3.8e-5)	-2.6e-3 (3.9e-4)

Table 3: Error with an Euler scheme with step $\delta = 0.1$ and finite difference approximation with step $dx = 0.4$. X^x is solution of (30), $N_{\text{MC}} = 1e9$, $M = 0.5$, $x = 0.04$. The program run 5.6e3 seconds.

$\Psi(y)$	$\hat{P}_\Psi(N_{\text{MC}}, \delta)$ $-P_\Psi$	$\hat{\Delta}_\Psi(N_{\text{MC}}, \delta, dx)$ $-\Delta_\Psi$	$\hat{\Gamma}_\Psi(N_{\text{MC}}, \delta, dx)$ $-\Gamma_\Psi$
y^2	4.5e-4 (1.8e-4)	3.6e-3 (9.3e-4)	-2.2e-3 (1.8e-2)
$\exp(-y)$	8.1e-5 (2.1e-4)	-1.1e-3 (1.1e-3)	-1.2e-3 (2.1e-2)
$\mathbb{1}_{y>x}$	6.8e-5 (7.1e-5)	2.7e-3 (3.5e-4)	-5.0e-4 (7.0e-3)

Table 4: Error with an Euler scheme with step $\delta = 0.005$ and finite difference approximation with step $dx = 0.2$. X^x is solution of (30), $N_{\text{MC}} = 5e7$, $M = 0.5$, $x = 0.04$. The program run 2.9e3 seconds.

In any cases, our algorithm is faster (10 to 100 times faster than the Euler scheme).

4.2 Symmetric modified Orstein-Uhlenbeck, convergence of the error of truncation

We test our unbiased algorithm to a second *toy* model. We only evaluate in this Section the error due to the truncation of the Poisson process. That is, we illustrate the results of Section 2.6. The comparison with an Euler scheme and finite difference approximation of the derivatives are very similar (in terms of complexity and on efficiency) to those obtained in the previous section. Thus, we do not include them for this example.

4.2.1 Introduction

We slightly modify the drift introduced in the previous example. In this part, we put

$$X_T^x = x + \int_0^T \alpha(X_t^x) dt + W_T$$

$$\alpha(x) = -M \left(x + \frac{1}{2} \right) \mathbb{1}_{x \leq -1} + \frac{M}{2} x^2 \mathbb{1}_{-1 \leq x \leq 1} + M \left(x - \frac{1}{2} \right) \mathbb{1}_{x \geq 1}. \quad (31)$$

Remark 6. For $y \leq 0$, the drift $\alpha(y)$ is identical to the drift in the previous example, but instead of putting $\alpha(y) = 0$ for $y \geq 0$, the drift is now symmetric. The associated function φ satisfies $\lim_{-\infty} \varphi = \lim_{+\infty} \varphi = +\infty$.

For any threshold K , we simulate the final value \tilde{B}_T^x , the minimum m of the Brownian bridge on $[0, T]$ and compute $\tilde{K}(\omega)$ according to (29). We then simulate a Poisson process N^K on $[0, T] \times [0, \tilde{K}(\omega)]$ and accept the path if $N^K \cap D(\omega) = \emptyset$, where $D(\omega)$ denotes the hypograph of $\varphi(\tilde{B}_t^x)$. We denote by $\tilde{X}_T^{x,K}$ the accepted values. We denote by p^K the probability to accept a Brownian bridge path (see (23)).

We use the notation $\tilde{P}_\Psi(N_{\text{MC}}, K)$ (resp. $\tilde{\Delta}_\Psi(N_{\text{MC}}, K)$, $\tilde{\Gamma}_\Psi(N_{\text{MC}}, K)$) for our Monte Carlo approximations of (2) (resp. (3), (4)), with a sample of size N_{MC} and a truncated Poisson process at level K .

4.2.2 Results

The result for $K = 100$ are given in Table 5 and are considered as benchmark.

$\Psi(y)$	$\tilde{P}_\Psi(N_{\text{MC}}, K)$	$\tilde{\Delta}_\Psi(N_{\text{MC}}, K)$	$\tilde{\Gamma}_\Psi(N_{\text{MC}}, 100)$
y^2	0.904526 (2.8e-5)	0.164247 (7.0e-5)	1.02012 (1.5e-4)
$\exp(-y)$	1.36243 (3.3e-5)	-1.08837 (8.7e-5)	0.564459 (2.2e-4)
$\mathbb{1}_{y>x}$	0.47637 (1.1e-5)	-0.357681 (1.4e-5)	-0.0531064 (2.6e-5)

Table 5: Results for the approximation $X_T^{x,K}$ of the solution of (31). $K = 100$, $M = 0.5$, $x = 0.04$, $N_{\text{MC}} = 2e9$. The program run 1.1e5 seconds.

In Tables 6, 7, 8, we can see the approximated biases for $K = 0, 1, 2$. We observe that according to Proposition 2, the bias decrease fast with K and the bias seems to be neglected for $K = 2$, even for the approximation of the derivatives.

Table 9 gives the empirical probability p^K to accept a Brownian bridge with the truncated algorithm at level K . It is obviously a monotonic function of K . We observe that $p^2 \approx p^{100}$ with a very large accuracy.

$\Psi(y)$	$\tilde{P}_\Psi(N_{\text{MC}}, K)$ $-\tilde{P}_\Psi(N_{\text{MC}}, 100)$	$\tilde{\Delta}_\Psi(N_{\text{MC}}, K)$ $-\tilde{\Delta}_\Psi(N_{\text{MC}}, 100)$	$\tilde{\Gamma}_\Psi(N_{\text{MC}}, K)$ $-\tilde{\Gamma}_\Psi(N_{\text{MC}}, 100)$
y^2	1.66e-2 (2.8e-5)	7.6e-4 (6.9e-5)	9.7e-3 (1.5e-4)
$\exp(-y)$	1.2e-3 (3.2e-5)	-4.9e-2 (8.6e-5)	1.9e-2 (2.2e-4)
$\mathbb{1}_{y>x}$	-8.0e-3 (1.1e-5)	-1.6e-2 (1.4e-5)	6.3e-3 (2.6e-5)

Table 6: Errors with the truncated approximation $X_T^{x,K}$ of the solution of (31). $K = 0$, $M = 0.5$, $x = 0.04$, $N_{\text{MC}} = 2e9$. The program run 1.1e4 seconds.

$\Psi(y)$	$\tilde{P}_\Psi(N_{\text{MC}}, K)$ $-\tilde{P}_\Psi(N_{\text{MC}}, 100)$	$\tilde{\Delta}_\Psi(N_{\text{MC}}, K)$ $-\tilde{\Delta}_\Psi(N_{\text{MC}}, 100)$	$\tilde{\Gamma}_\Psi(N_{\text{MC}}, K)$ $-\tilde{\Gamma}_\Psi(N_{\text{MC}}, 100)$
y^2	1.0e-4 (2.8e-5)	4.1e-4 (7.0e-5)	-9.5e-3 (1.5e-4)
$\exp(-y)$	1.0e-5 (3.3e-5)	1.4e-4 (8.7e-5)	-6.3e-3 (2.2e-4)
$\mathbb{1}_{y>x}$	1.6e-5 (1.1e-5)	5.0e-6 (1.4e-5)	6.0e-4 (2.6e-5)

Table 7: Results for the approximation $X_T^{x,K}$ of the solution of (31). $K = 1$, $M = 0.5$, $x = 0.04$, $N_{\text{MC}} = 2e9$. The program run 1.2e4 seconds.

$\Psi(y)$	$\tilde{P}_\Psi(N_{\text{MC}}, K)$ $-\tilde{P}_\Psi(N_{\text{MC}}, 100)$	$\tilde{\Delta}_\Psi(N_{\text{MC}}, K)$ $-\tilde{\Delta}_\Psi(N_{\text{MC}}, 100)$	$\tilde{\Gamma}_\Psi(N_{\text{MC}}, K)$ $-\tilde{\Gamma}_\Psi(N_{\text{MC}}, 100)$
y^2	6e-6 (2.8e-5)	-2.7e-5 (7.0e-5)	2.2e-4 (1.5e-4)
$\exp(-y)$	1.0e-5 (3.3e-5)	-1.0e-5 (8.7e-5)	4.2e-5 (2.2e-4)
$\mathbb{1}_{y>x}$	1.9e-5 (1.1e-5)	-9e-6 (1.4e-5)	-1.5e-5 (2.6e-5)

Table 8: Results for the approximation $X_T^{x,K}$ of the solution of (31). $K = 2$, $M = 0.5$, $x = 0.04$, $N_{\text{MC}} = 2e9$. The program run 1.3e4 seconds.

4.3 CIR

In this Section, we present the numerical results obtained for the simulation of the CIR, solution of (27) (see Section 3. The numerical experiments are computed with parameters $\kappa = 0.5$, $V_\infty = 0.04$, $\varepsilon = 0.1$, $T = 1$ and the initial condition $v = 0.04$). The algorithm differs from the two previous examples. We first apply the Lamperti transform and simulate $X_t^x = \eta(V_t^v)$ with our (almost) unbiased algorithm (with $x = \eta(v)$). Then, for any function Ψ , we use the approximation $\tilde{P}_\Psi^X(x, N_{\text{MC}})$, $\tilde{\Delta}_\Psi^X(x, N_{\text{MC}})$ and $\tilde{\Gamma}_\Psi^X(x, N_{\text{MC}})$ constructed for the process X^x . We deduce the corresponding approximation for the CIR

$$\bar{P}_\Psi^V(v, N_{\text{MC}}) = \tilde{P}_\Psi^X(\eta(v), N_{\text{MC}}) \quad (32)$$

$$\bar{\Delta}_\Psi^V(v, N_{\text{MC}}) = \eta'(v) \tilde{\Delta}_\Psi^X(\eta(v), N_{\text{MC}}) \quad (33)$$

$$\bar{\Gamma}_\Psi^V(v, N_{\text{MC}}) = \eta'(v)^2 \tilde{\Gamma}_\Psi^X(\eta(v), N_{\text{MC}}) + \eta''(v) \tilde{\Delta}_\Psi^X(\eta(v), N_{\text{MC}}). \quad (34)$$

Description of the compared algorithms We first (see 0-) remind the quantities we aim to estimate. Then, we descript the four algorithms we numerically compare in this Section. We explain the different quantities we compare in this Section

0- The exact values are denoted by $P_\Psi(v)$, $\Delta_\Psi(v)$ and $\Gamma_\Psi(v)$, that is

$$\begin{aligned} P_\Psi(v) &= \mathbb{E}\Psi(V_T^v) \\ \Delta_\Psi(v) &= \frac{d}{dv} \mathbb{E}\Psi(V_T^v) \\ \Gamma_\Psi(v) &= \frac{d^2}{dv^2} \mathbb{E}\Psi(V_T^v). \end{aligned}$$

K	0	1	2	100
p^K	0.877731	0.832898	0.832884	0.832877

Table 9: Probability p^K defined in (23) to accept a Brownian bridge path.

$\Psi(y)$	P_Ψ	$\bar{P}_\Psi(N_{MC}^1) - P_\Psi$	$\hat{P}_\Psi(N_{MC}^2, \delta^1) - P_\Psi$	$\hat{P}(N_{MC}^2, \delta^2) - P_\Psi$
y	0.04	-4.5e-9 (1.6e-8)	7e-7 (5.0e-7)	2e-7 (5.1e-7)
$\mathbb{1}_{y>v}$	0.545628	0 (5.0e-7)	2.5e-4 (1.8e-5)	3.1e-3 (1.6e-5)
$\exp(-y)$	0.960910476	1e-9 (1.5e-8)	1.2e-7 (4.8e-7)	6e-6 (4.9e-7)

Table 10: Estimation of the error (reference in bold) on the expectation and the corresponding standard deviation for the CIR with different methods. $N_{MC}^1 = 1e12$, $N_{MC}^2 = 1e9$, $\delta^1 = 0.001$, $\delta^2 = 0.1$.

- 1- Our approximations $\bar{P}_\Psi(N_{MC})$, $\bar{\Delta}_\Psi(N_{MC})$ and $\bar{\Gamma}_\Psi(N_{MC})$ are defined in (32), (33) and (34).
- 2- The approximations using an Euler scheme and finite difference approximation are denoted $\hat{P}_\Psi(N_{MC}, \delta)$, $\hat{\delta}_\Psi(N_{MC}, \delta, dv)$ and $\hat{\Gamma}_\Psi(N_{MC}, \delta, dv)$ (see Sec. 4.1.3).
- 3- We also approximate with an Euler scheme the expression of the derivatives obtained after the Malliavin integration by part (see Section 2.2 and 2.3): $\bar{\Delta}_\Psi(N_{MC}, \delta)$ and $\bar{\Gamma}_\Psi(N_{MC}, \delta)$.
- 4- Finally, we approximate Δ_Ψ and Γ_Ψ thanks to the finite difference approximation applied to our unbiased estimators of $\bar{P}_\Psi^v(N_{MC})$, $\bar{P}_\Psi^{v-dv}(N_{MC})$ and $\bar{P}_\Psi^{v+dv}(N_{MC})$. We will denote these approximations as $\tilde{\Delta}_\Psi(N_{MC}, dv)$ and $\tilde{\Gamma}_\Psi(N_{MC}, dv)$.

The results and the corresponding standard deviations of these estimators (with the truncated algorithm at level $K = 20$) are given in Tables 10, 11 and 12. We put in bold symbols the exact theoretical results when they are available. For the function $\Psi = \mathbb{1}_{y>v}$, we have put in the reference column (P_Ψ , Δ_Ψ , Γ_Ψ) the approximation with our methods with a sample of size $N_{MC} = 1e12$.

Discussion on the results In any column, except the third one, we observe bias for the non smooth function $\Psi(y) = \mathbb{1}_{y>v}$. Moreover, the variance of our algorithm is comparable to the variances of the biased one. In a fixed time devoted for simulation, our unbiased algorithm is always the most precise one in these examples.

Control of the error Even if the rigorous proof presented in Section 2.6 can not be directly used for the CIR process, a similar control of the error for the truncated algorithm should be obtained. For $K = 20$ and the bounded function Ψ case ($\Psi(y) = \mathbb{1}_{\{y>v\}}$), we obtained an accuracy of order $1e - 100$.

Ψ	Δ_Ψ	$\bar{\Delta}_\Psi(N_{MC}^1)$ $-\Delta_\Psi$	$\hat{\Delta}_\Psi(N_{MC}^2, \delta^1)$ $-\Delta_\Psi$	$\check{\Delta}_\Psi(N_{MC}^3, \delta^2, dv)$ $-\Delta_\Psi$	$\tilde{\Delta}_\Psi(N_{MC}^3, dv)$ $-\Delta_\Psi$
y	0.606531	1e-6 (6.5e-6)	3.0e-3 (6.3e-5)	7.8e-3 (5.1e-5)	2e-6 (4.2e-5)
$\mathbb{1}_{y>v}$	-15.3247626	0 (8.5e-5)	-4.3e-2 (7.4e-4)	-8.0e-1 (1.5e-3)	-0.32 (1.3e-3)
$\exp(-y)$	-0.58053743	-2.1e-7 (1.3e-4)	6.2e-2 (1.2e-3)	7.6e-3 (4.9e-5)	-2e-6 (4.0e-5)

Table 11: Estimation of the first derivatives and the corresponding standard deviation for the CIR with different methods. $N_{MC}^1 = 1e12$, $N_{MC}^2 = 1e9$, $N_{MC}^3 = 1e10$, $\delta^1 = 0.001$, $\delta^2 = 0.1$, $dv = 0.01$

Ψ	Γ_Ψ	$\bar{\Gamma}_\Psi(N_{MC}^1)$ $-\Gamma_\Psi$	$\hat{\Gamma}_\Psi(N_{MC}^2, \delta^1)$ $-\Gamma_\Psi$	$\check{\Gamma}_\Psi(N_{MC}^3, \delta^2, dv)$ $-\Gamma_\Psi$	$\tilde{\Gamma}_\Psi(N_{MC}^3, dv)$ $-\Gamma_\Psi$
y	0	-5.1e-4 (1.9e-3)	-4.0e-2 (4.0e-3)	3.7e-4 (2.0e-2)	-1.1e-2 (1.7e-2)
$\mathbb{1}_{y>v}$	12 (6.2e-1)	-7.1 (5.2e-1)			
$\exp(-y)$	0.35073	-3.1e-3 (3.6e-2)	-4.6e-1 (6.9e-2)	-1.0e-2 (2.0e-2)	1.0e-2 (1.6e-2)

Table 12: Estimation of the second derivative and the corresponding standard deviation for the CIR with different methods. $N_{MC}^1 = 1e12$, $N_{MC}^2 = 1e9$, $N_{MC}^3 = 1e10$, $\delta^1 = 0.001$, $\delta^2 = 0.1$, $dv = 0.01$

5 Conclusion

In this work, we slightly improved the Beskos et al. [2] exact method to simulate the solution of one dimensional SDEs. We simulated the Poisson process useful to reject the Brownian bridge paths in a more efficient order (by increasing ordinates). It also allowed us to extend the methodology to more general drift functions α . In this case, we obtained a control of the error due to the truncation of the Poisson process.

In addition, we proposed to generalise the unbiased Monte Carlo algorithm to the estimation of the derivatives (3) and (4).

In comparison with the previous classical numerical methods, our algorithm seems to be more efficient if we want to obtain a sufficiently good accuracy. For rough approximations, the bias introduced by Euler scheme has the same order as the statistical error of our algorithm.

References

- [1] A. Alfonsi. *Affine diffusions and related processes: simulation, theory and applications*, volume 6 of *Bocconi & Springer Series*. Springer, Cham; Bocconi University Press, Milan, 2015.
- [2] A. Beskos, O. Papaspiliopoulos, and G. O. Roberts. Retrospective exact simulation of diffusion sample paths with applications. *Bernoulli*, 12(6):1077–1098, 2006.
- [3] A. Beskos and G. O. Roberts. Exact simulation of diffusions. *Ann. Appl. Probab.*, 15(4):2422–2444, 2005.

- [4] L. Devroye. *Nonuniform random variate generation*. Springer-Verlag, New York, 1986.
- [5] E. Fournié, J.-M. Lasry, J. Lebuchoux, P.-L. Lions, and N. Touzi. Applications of Malliavin calculus to Monte Carlo methods in finance. *Finance Stoch.*, 3(4):391–412, 1999.
- [6] I. Karatzas and S. E. Shreve. *Brownian motion and stochastic calculus*, volume 113 of *Graduate Texts in Mathematics*. Springer-Verlag, New York, second edition, 1991.
- [7] S. Maire and E. Tanré. Some new simulations schemes for the evaluation of Feynman-Kac representations. *Monte Carlo Methods Appl.*, 14(1):29–51, 2008.
- [8] D. Nualart. *The Malliavin calculus and related topics*. Probability and its Applications (New York). Springer-Verlag, Berlin, second edition, 2006.
- [9] D. Williams. Path decomposition and continuity of local time for one-dimensional diffusions. I. *Proc. London Math. Soc. (3)*, 28:738–768, 1974.

Victor Reutenauer

Fotonower
 30 rue Charlot
 F-75003 Paris
victor@fotonower.com

Etienne Tanré

Université Côte d’Azur, Inria, France.
 Team Tosca
 2004, route des Lucioles, BP 93
 F-06902 Sophia Antipolis Cedex
Etienne.Tanre@inria.fr